Photon Correlation Spectroscopy

James Amarel and Adeel Ali

April 18, 2017

1 Goal

To determine the radius of micro-spheres in thermodynamic equilibrium with a fluid through measurement of their translational diffusion coefficient, which is dependent on the micro-sphere radius due to Stokes' drag law, and is extracted from the correlation function of the time dependent intensity of light reflected off the suspension.

2 Introduction/Background

A fluid medium, composed of individual molecules, exerts a stochastic force upon embedded microscopic particles, causing what is known as Brownian motion. Under random bombardment by fluid molecules, these larger particles perform a random walk, where a new direction is chosen upon each collision, ultimately leading to a nonzero mean squared displacement for an average over a large number of particles.

According to the equipartition theorem, particles in equilibrium with a thermodynamic system carry a nonzero kinetic energy that is dependent upon the number of degrees of freedom and temperature. Due to the large relative size between microparticles and fluid molecules, the embedded spheres experience a viscous resistance proportional to their radius and velocity, which, as shown by Langevin [2], characterize the translational diffusion coefficient

$$D_T = \frac{k_B T}{6\pi\eta r} \tag{1}$$

where k_B is Boltzmann's constant, T is the system temperature, η is the fluid viscosity, and r is the particle radius.

The motion of such spherical particles can be studied through the process of dynamic light scattering. Fluctuations in the intensity of light scattered from the microparticles, due to their constant state of agitation, is statistically linked to particle movement. For plane waves of wavenumber $\vec{k}_i$ incident on an isotropic particle suspension, with coordinates such that the j'th particle is at location $\vec{r}_j$, light is reflected from each particle, of which a portion, carrying wavenumber $\vec{k}_s$, interferes at a detector, creating a net electric field that can be expressed

$$\mathbf{E}_s = \sum_{j=1}^{N} \mathbf{E}_j \tag{2}$$

where $\mathbf{E}_j$ is the field due to the j'th particle, out of N particles, where

$$\mathbf{E}_j = \mathbf{E}_o e^{-i(\omega t + \phi_j)} \tag{3}$$

for amplitude E_o, which is constant for all contributions, since the scattering centers are identical spheres, angular frequency ω, and phase constant ϕ_j. Note ϕ_j is the phase accumulated due to reflection from position $\vec{r}_j$, where light reflected from the origin is chosen to have phase $\phi_{origin} = 0$. As seen in Figure 1, each particle will scatter light in the direction of the detector after advancing in phase an amount $\mathbf{k}_i \cdot \mathbf{r}_j$ to reach their target. Then, by accounting for the linear distance from the scattering source to the detector, we find

$$\phi_j = \vec{k}_i \cdot \vec{r}_j - \vec{k}_s \cdot \vec{r}_j = \vec{K} \cdot \vec{r}_j \tag{4}$$

where $\vec{K} = \vec{k}_i - \vec{k}_s$. Photons reflected from the microspheres experience an energy loss sufficiently small for the approximation $k_i = k_s$, which allows the law of cosines relationship for the magnitude of $\vec{K}$

$$|\vec{K}| = \frac{4\pi n}{\lambda_o} \sin\frac{\theta_s}{2} \tag{5}$$

where n is the refractive index of the medium, λ_o is the wavelength of the incident light when in vacuum, and θ_s is the scattering angle.

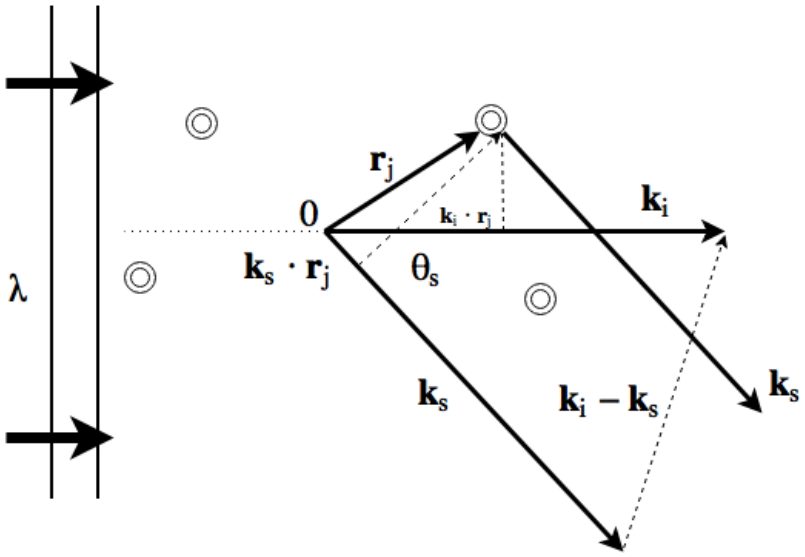

Figure 1: A plane wave of wavelength λ and wavevector $\vec{k}_i$ encounters a spherical particle at $\vec{r}_j$, producing a scattered wave of wavevector $\vec{k}_s$, which travels towards a detector mounted at angle θ_S from $\vec{k}_i$.

By the Weiner-Khintchine theorem, a well behaved wide-sense stationary random process, such as the intensity fluctuations described above, can be expressed as the power spectrum

$$I(\omega) = \frac{1}{2\pi} \int_{-\infty}^{\infty} C(\tau) e^{i\omega t}\, d\tau \tag{6}$$

where $C(\tau)$ is defined to be the autocorrelation function

$$C(\tau) = \langle E_s^\star(t) E_s(t+\tau) \rangle \tag{7}$$

Following the analysis of Cummings [1], approximation of the particle positions as being statistically independent (they are non-interacting), in combination with their spherical symmetry, reduces Equation 7 to the form

$$C(\tau) = Ae^{-2D_T K^2 \tau} \tag{8}$$

where D_T is the diffusion coefficient of the suspended particles, and A is an undetermined constant that depends on system parameters such as the light source, collection optics, and homogeneity of the spheres. At this point, Equation 6 can be evaluated analytically

$$I(\omega) = \delta(\omega) + \frac{2D_T K^2}{(2D_T K^2)^2 + \omega^2}. \tag{9}$$

where $\delta(\omega)$ is the delta distribution function centered about $\omega = 0$. Equation 9 is a Lorentzian centered about the origin, with a HWHM of $2D_T K^2$, where typical values of D_T and K for this setup are of order 10^{-11} $m^2 s^{-1}$ and 10^7 m^{-1}, respectively. Therefore, the spectrum of intensity fluctuations in the frequency domain is of width kHz, removing the need for high precision instruments capable of detecting broadening centered about the source frequency, which is of order 10^{14} for an HeNe laser.

3 Procedures and Data

In practice, the intensity of light reflected from nanoparticles is sufficiently low that only photon counting techniques are equipped to detect any time or frequency variations in the intensity. We aimed an HeNe laser, as seen in Figure 2, at a suspension of nanospheres in a cuvette, then collected light reflected at 90^o with a fiber optic cable and fed that information to a correlator, which, through the computer, returned the value of $C(\tau)$ for a set of lag times τ in the interval from 1 μs to 10^5 μs. Fortunately, correlator devices are readily made with the ability to quickly compute a correlation function in intensity, which can then be compared with Equation 8 to determine the diffusion coefficient.

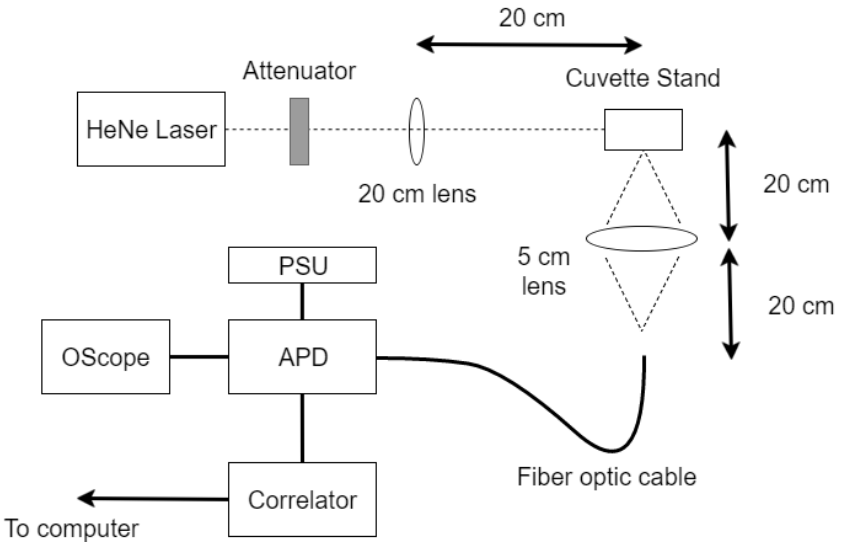

Figure 2: Block diagram of the experimental apparatus.

To regulate the signal intensity, we used an attenuator, two focusing lenses, and an avalanche photo diode, which amplifies the electrical signal through an electron cascade. We first measured the dark count rate to be 1.3 kcps, and then adjusted the attenuator such that the count rate due to reflection off a 0.11 μm sphere suspension in DI water was on order 80 kcps, ensuring that the dark count rate was negligible. Then, after positioning the cuvette to allow only light scattered at $90^o \pm 2$ from particles in the central area of the suspension to reach the detector (reducing boundary effects on diffusion), we instructed the correlator to record the intensity as a function of time for a time $T = 2$ minutes, from which it computes the correlation function

$$C(\tau) = \frac{1}{T} \int_0^T I(t) I(t + \tau) d\tau \tag{10}$$

as a digital approximation, which can be used in place of Equation 7, where $I(t)$ is the light intensity as a function of time. A plot of one such result is shown in Figure 3, where the signal is highly correlated for short lag times, corresponding to the fact that in a Brownian process, the particles are likely to increment to a state that is reasonably similar to its previous one, and displays effectively zero correlation for large lag times, eventually the system loses its memory. For particles of large D_T, the correlation decays faster, which is as expected for particles with a larger mean squared displacement.

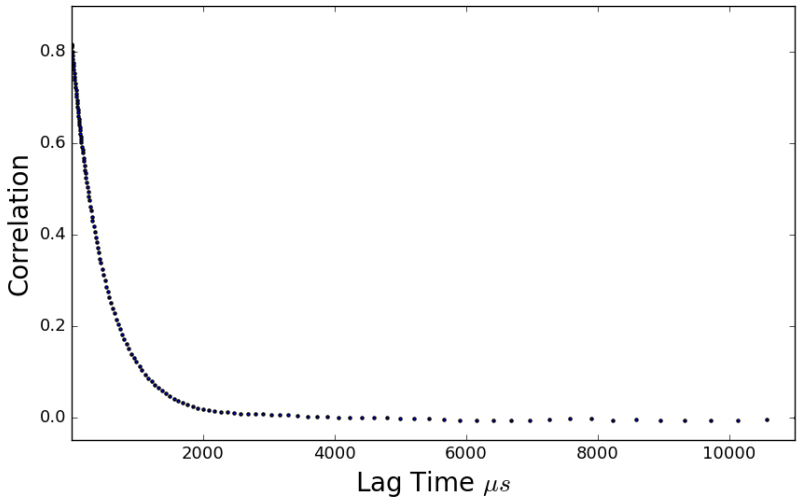

Figure 3: Digitally approximated correlation function of Lorentzian shape due to reflection off 0.11 μm spheres immersed in DI water.

In total, we measured the correlation function for four different situations: 0.11 μm spheres immersed in DI water, 1.53 μm spheres immersed in DI water, 0.11 μm spheres immersed in an 80% DI water - 20% Glycerine (by wt.) solution, and both 0.11 μm and 1.53 μm spheres immersed in DI water. By introducing Glycerine, we can investigate how diffusion changes and whether this model is consistent across fluids of different viscosity. Measurements of the diffusion coefficient in the two particle scenario, when compared with their corresponding single particle results, may provide indirect evidence as to the strength of interaction between the dislike spheres.

When preparing our samples, we diluted them to the point where 30% of the laser intensity was lost upon passing through the cuvette, such that reflected light reaching the detector was unlikely to have undergone two reflections, and placed the sample in an ultrasonic bath to ensure a proper particle distribution.

4 Analysis and Discussion

In order to extract the diffusion coefficient for the single particle correlation functions $C(\tau)$, we performed a linear fit to the relationship $\ln(C(\tau)) = \ln A - 2D_T K^2 \tau$, which is shown for in Figures 4 - 6, where the refractive index n was 1.33 for DI water, and 1.375 for our glycerine solution. In the case of 0.11 μm beads in DI water, we found $D_{T1} = (2.83 \pm 0.006) \times 10^{-12}\ m^2 s^{-1}$, a value about ten times that of our 1.53 μm in DI water result of $D_{T2} = (0.227 \pm 0.002) \times 10^{-12}\ m^2 s^{-1}$, which means, as is intuitively expected for increasing inclusion size, the larger particles are less free to diffuse about the medium. At room temperature $T = 293K \pm 3$, the viscosity of DI water is $\eta_{DI} = 1.005$ mPa, and the viscosity of a 20% glycerine solution is $\eta_{Sol} = 1.76$ mPa, which allows computation of the particle radius through Equation 1, where we find $r_1 = 0.7552 \pm 0.00015\ \mu m$ and $r_2 = 0.94214 \pm 0.00639\ \mu m$, both of which are on the same order as the labeled particle radii of 0.055 μm and 0.765 μm, respectively, but are many standard deviations larger than expected. This discrepancy is unlikely to have been caused by error recording in the scattering angle or temperature, as both weakly effect the value of D_T, but may have been introduced by a 10% decrease in the refractive index n, a quantity that we estimated from a tabulated value for light of wavelength 589 nm. Another possibility is that the cuvette inhibited the particle ability for free diffusion.

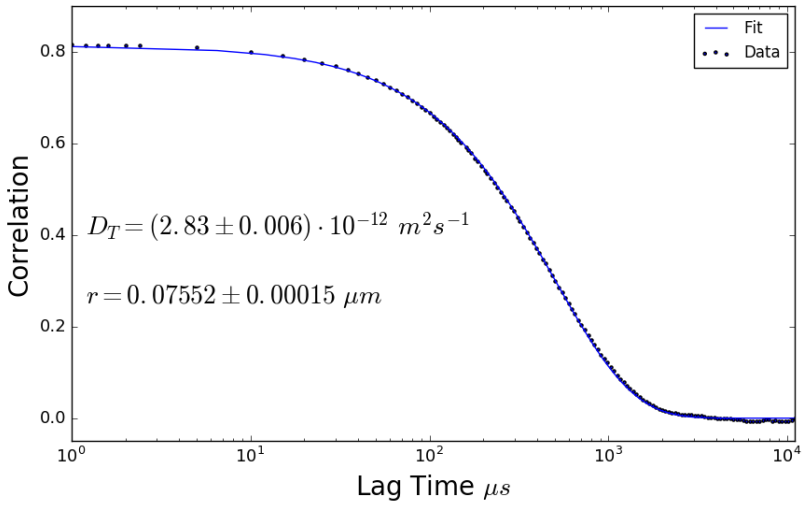

Figure 4: Log scale results of a linear fit to the correlation function of reflection off 0.11 μm spheres immersed in DI water.

With the introduction of glycerol, seen in Figure 6, we expect the mobility of 0.11 μm particles to be reduced, which is reflected by a reduction in the diffusion coefficient for 0.11 μm beads to $D_T = (1.561 \pm 0.005) \times 10^{-12}\ m^2 s^{-1}$, an approximately

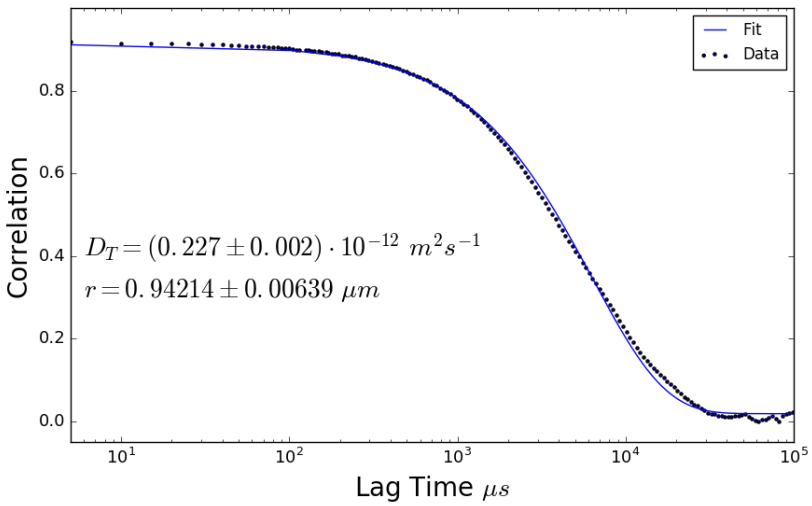

Figure 5: Log scale results of a linear fit to the correlation function of reflection off 1.53 μm spheres immersed in DI water.

50% from the purely DI water scenario. In this case, we found the particle radius to be $r_1' = 0.7814 \pm 0.0024\ \mu m$, which is similar to our measurements with neat DI water, which suggests the model is reasonably self consistent, although there is some discrepancy between measurements of the same particles in different mediums, which may be the result of stronger interactions between the particles in a more viscous environment.

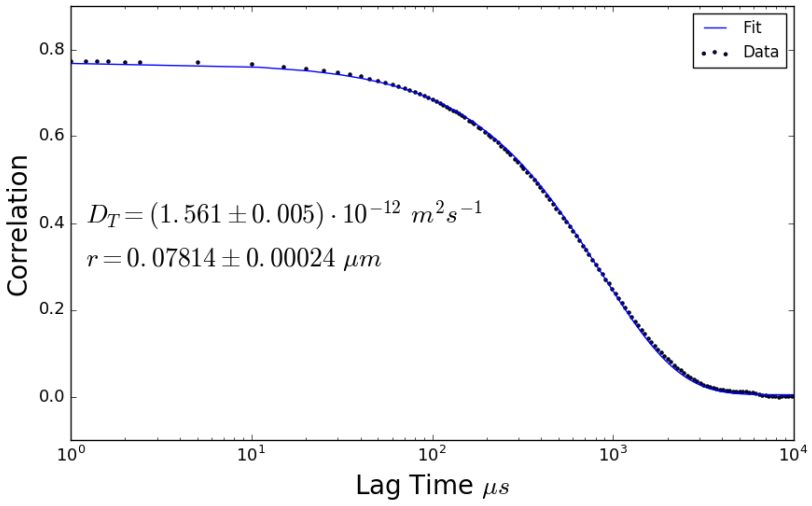

Figure 6: Log scale results of a linear fit to the correlation function of reflection off 0.11 μm spheres immersed in an 80% DI water - 20% glycerine (by wt.) solution.

In the final scenario of 0.11 μm and 1.53 μm spheres immersed in DI water, there are competing signatures in the correlation function, thus we abandon the linear fitting method and perform a fit, as seen in Figure 7, of the form

$$C(\tau) = Ae^{-2D_{T1}K^2\tau} + Be^{-2D_{T2}K^2\tau} \tag{11}$$

where A and B are proportionality fitting factors, D_{T1} is the diffusion coefficient of the 0.11 μm particles, and D_{T1} is the diffusion coefficient of the 1.53 μm particles. Here we find significantly different values than in the single particle case, indicating there is definite interaction between the particles, where $D_{T1} = (4.361 \pm 0.166) \times 10^{-12}$ $m^2 s^{-1}$ and $D_{T2} = (2.263 \pm 0.047) \times 10^{-12}$ $m^2 s^{-1}$, which are approximately twice that of their corresponding single particle diffusion rate. Since the Langevin model is not equipped to handle multi-particle interactions, our measured values for the particle radii, $r_1 = 0.4896 \pm 0.00186$ μm and $r_2 = 0.09438 \pm 0.00195$ μm, are in disagreement with the labeled radii.

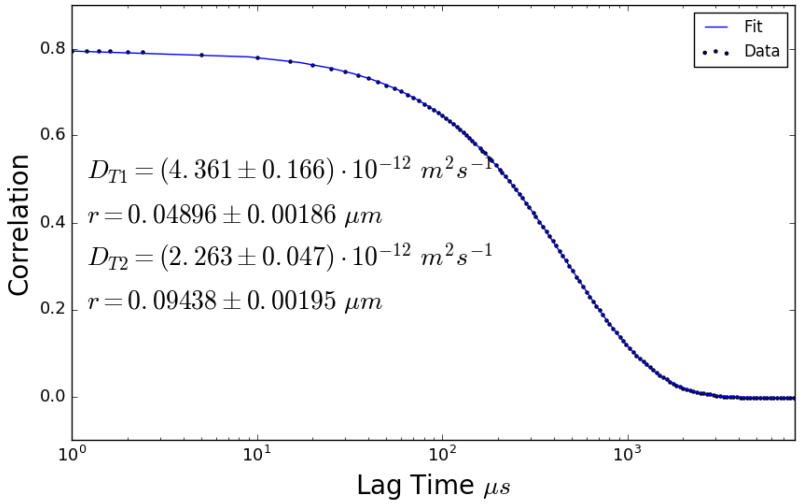

Figure 7: Log scale results of a nonlinear linear fit to the correlation function of reflection off 0.11 μm and 1.53 μm spheres immersed in DI water.

5 Conclusion

We have shown that the kinetic transfer of heat from a fluid medium to microscopic particles embedded within will lead to a nonzero mean squared displacement of the particles over a time interval τ. This follows from the fact that if a particle experiences a force in a random direction (say left or right) then there is only a fractional percentage (50%) that the particle will be returned to its previous location on the next collision. Dynamic light scattering techniques provide a way to infer information about the motion of particles exhibiting Brownian motion due to the interference of light rays scattered from the particles. Through the Weiner-Khintchine theorem, and the Langevin equation, one can relate the intensity fluctuations to the diffusion coefficient of the particles, which is a quantity that depends on the particle radius.

By measuring the diffusion coefficient, which was of order 10^{-12} for all samples, we determined the radius of a set of particles embedded within a fluid medium of various viscosity for the case of single and two particle suspensions. Our samples were prepared with 0.055 μm and/or 0.765 mum micro-spheres, which we measured to have

radii 0.07552 ± 0.00015 μm and 0.94214 ± 0.00639 μm. Our results were in agreement to the order of magnitude, but were consistently larger than their expected values. By performing measurements of multi-particle suspensions, we found significant changes in the measured values of the diffusion coefficient, suggesting hard interactions between the particles, and revealing that this model does not account for interacting particles.

References

[1] H Z Cummins, F D Carlson, T J Herbert, and G Woods. Translational and rotational diffusion constants of tobacco mosaic virus from Rayleigh linewidths. *Biophysical journal*, 1969. ISSN 0006-3495. doi: 10.1016/S0006-3495(69)86402-7.

[2] D Lemons and A Gythiel. Paul Langevins 1908 paper On the Theory of Brownian Motion. *American Journal of Physics*, 65(11), 1997.